Journal of Chromatography, 600 (1992) 297–304
Elsevier Science Publishers B.V., Amsterdam

CHROM. 24 073

Isoelectric focusing field-flow fractionation

III. Investigation of the influence of different experimental parameters on focusing of cytochrome *c* in the trapezoidal cross-section channel

Josef Chmelík*

Institute of Analytical Chemistry, Czechoslovak Academy of Sciences, Veveří 97, CS-611 42 Brno (Czechoslovakia)

Wolfgang Thormann

Department of Clinical Pharmacology, University of Berne, Murtenstrasse 35, CH-3010 Berne (Switzerland)

(First received October 22nd, 1991; revised manuscript received February 3rd, 1992)

ABSTRACT

In addition to the electric field and pH gradient used in isoelectric focusing, a recently introduced technique, isoelectric focusing (or electrical hyperlayer) field-flow fractionation, employs the flow of the liquid carrier through a thin separation channel as a third factor affecting separation. Focusing of cytochrome *c* (CYTC) in a trapezoidal cross-section channel of 0.875 ml volume and 25 cm length was investigated as a function of the injection procedure, relaxation time, flow-rate of the carrier ampholyte solution and applied electric power. The influence of different initial conditions was also investigated by computer simulation. Both computed and experimental data showed an important contribution of the injection procedure and relaxation time on the retention and shape of the CYTC zone. It follows from these data that the sample should be injected as a narrow zone into the centre of the stream rather than homogeneously together with the carrier solution. For the described experimental set-up it could be demonstrated that the time necessary for zone formation should be at least 15 min and that relaxation times in excess to 20 min do not influence the final shape of the CYTC zone. It could further be shown experimentally that the sample must be injected under an applied electric field, that the relaxation time should be about 10 min, that the elution flow-rate should not be larger than 100 μl/min, that focusing becomes more efficient with increasing electric fields and that, for a given assembly and specified flow conditions, there is an electric power window only within which proper operation is possible.

INTRODUCTION

Isoelectric focusing field-flow fractionation (IEF_4) is a technique for the separation of ampholytes using the combination of an electric field, a pH gradient and a flow velocity profile whose shape is determined by the geometry of the separation channel [1–3]. Amphoteric solutes are transported via isoelectric focusing to the equilibrium positions, where these compounds possess no net overall charge, and narrow focused solute zones with nearly Gaussian concentration distributions are formed. Provided that solutes exhibit different isoelectric points, they focus in different positions across the separation channel. Unequal flow velocities (Fig. 1A) cause differential migration of focused solutes along the channel, *i.e.*, their longitudinal separation.

IEF_4 was experimentally introduced by Chmelík *et al.* [2] in the trapezoidal cross-section channel and

0021-9673/92/$05.00

by Thormann *et al.* [3] in the rectangular cross-section channel. The latter group named this technique electrical hyperlayer field flow fractionation following the terminology of Giddings [4]. The formation of the pH gradient [5] and IEF_4 of a low-molecular-mass compound (methyl red) in the trapezoidal cross-section channel [6] have also been studied. This work was concerned with IEF_4 of a high-molecular-mass amphoteric compound, cytochrome *c* (CYTC), in the trapezoidal cross-section channel. The influence of different experimental parameters, including sample injection, relaxation, elution flow-rate and power, on the retention and zone width of CYTC is reported. The focusing process for two sample injection procedures was investigated both experimentally and by computer simulation using a mathematical model developed for electrophoretic processes [7,8].

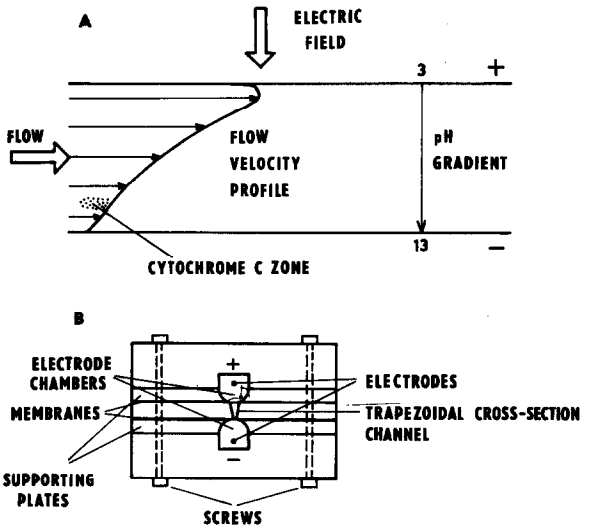

Fig. 1. Schematic representation of (A) IEF_4 in the trapezoidal cross-section channel and (B) cross-section of the IEF_4 channel assembly.

EXPERIMENTAL

Chemicals

All chemicals were of analytical-reagent grade. Cytochrome *c* from horse heart (M_r = 12 384, p*I* = 9.3) was obtained from Sigma (St. Louis, MO, USA) and Ampholine (pH 3.5–10) from Pharmacia–LKB (Bromma, Sweden).

Instrumentation and experimental conditions

The scheme of the experimental IEF_4 arrangement with the trapezoidal cross-section channel has been published elsewhere [6]. A schematic representation of the flow velocity profile and a cross-sectional view of the IEF_4 cell assembly are shown in Fig. 1A and B, respectively. The length of the channel was 25 cm, the height was 0.5 cm and the lengths of the two opposite walls of the trapezoid were 0.45 and 0.95 mm (volume 0.875 ml). Two additional Perspex plates were used for the mounting of PLGC ultrafiltration membranes (Millipore, Bedford, MA, USA) and to avoid changes in the channel flow conditions. For trouble-free operation the channel was run with the electrode compartments sideways, *i.e.*, turned 90°C with respect to Fig. 1B. A two-channel peristaltic pump (Vario Perpex, H. J. Guldener, Zürich, Switzerland) was used to pump 0.1 *M* acetic acid and 0.1 *M* sodium hydroxide solution through the electrode chambers, each at a flow-rate of 250 μl/min. A Model 2150 high-performance liquid chromatographic (HPLC) pump (LKB, Bromma, Sweden) was employed to pump 0.5% (w/v) carrier ampholyte solution through the IEF_4 channel at a flow-rate in the range 10–200 μl/min. A Model 355 syringe pump (Sage Instruments, Cambridge, MA, USA) was used to introduce the sample, $5 \cdot 10^{-5}$ *M* CYTC in 0.5% Ampholine solution.

Employing a four-port valve with a 5-μl sample loop, two ways of sample introduction were studied (Fig. 2). In one, sample was slowly admitted through a capillary situated 2 cm downstream from the carrier inlet (Fig. 2B). In the other experimental arrangement (Fig. 2A), the sample was introduced through the carrier stream. In this instance the four-port valve was located between the HPLC pump and the carrier inlet capillary. In all instances the carrier flow-rate during injection was 10 μl/min. Eluting zones were monitored with a Model 2158 Uvicord SD photometric detector (LKB) at 405 or 280 nm and a Model 2210 recorder (LKB). A Model 2297 Macrodrive 5 power supply (LKB) was used to apply up to 20 V (the maximum current was *ca.* 150 mA). In most instances the total electric power was limited to 1 W to avoid deleterious electrohydrodynamic effects [9].

Concentrations of ampholyte, sample and electrode solutions were chosen on the basis of previous

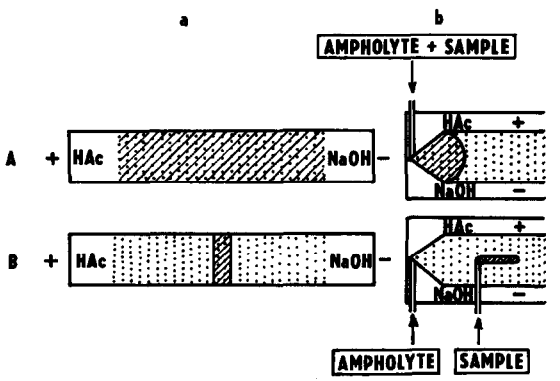

Fig. 2. Comparison of two sample introduction schemes for IEF_4. (A) Homogeneous sample distribution after injection of the sample together with the ampholyte solution through the carrier inlet. (B) Pulse sample distribution after injection of the sample through the capillary located 2 cm downstream of the carrier inlet. Initial distribution of compounds used for computer simulation and experiments are shown in (a) and (b), respectively. The dotted areas show the distribution of carrier ampholytes and the hatched areas depict the distribution of CYTC.

measurements [5,6]. Unless stated otherwise, the sample (5 μl of $5 \cdot 10^{-5}$ *M* CYTC) was injected over a period of 4 min with power applied and a carrier flow-rate of 10 μl/min. Relaxation, *i.e.*, the formation of a focused zone under this reduced flow-rate, occurred either within the flowing stream or, for relaxation times longer than 10 min, under stop-flow conditions. The zones were then eluted from the channel at a flow-rate of 40, 100 or 200 μl/min. The carrier ampholyte and sample solutions were degassed by vacuum and filtered through 0.2-μm Nalgene (25-mm diameter) disposable syringe filters (Nalge, Rochester, NY, USA).

Computer simulation

For simulation, the PC-adapted software package of the transient electrophoretic model developed by Bier *et al.* [7] was employed. This model is one-dimensional and isothermal and assumes the absence of fluid flows. For this reason, simulation does not describe separation in IEF_4 but focusing at zero or very low flow-rates without elution. Briefly, the model is capable of treating biprotic ampholytes, weak and strong monovalent acids and bases, peptides and proteins. Component fluxes result from electromigration and diffusion. It predicts the concentration distribution of individual components, pH and conductivity profiles as a function of time. The input required includes pK and mobility values of each component, the length of the separation space and its segmentation, the electrophoresis time, the current density, the initial distribution of each component and a table of net charge *versus* pH and also the diffusion coefficient for each protein. The permeabilities of the ends of the separation space are also specified. Simulations were performed on a Mandax AT 286 personal computer.

Ten biprotic carrier ampholytes were used to establish a pH gradient between acetic acid and sodium hydroxide. The pI values uniformly span the range 3–12 (ΔpI = 1). For each ampholyte, ΔpK was 2, the ionic mobility was $3 \cdot 10^{-8}$ m^2/V · s and the initial concentration was $2 \cdot 10^{-3}$ *M*. The concentrations of acetic acid (pK = 4.76) and sodium hydroxide solution were 0.1 *M* and the mobilities of acetate and sodium were $4.12 \cdot 10^{-8}$ and $5.19 \cdot 10^{-8}$ m^2/V · s, respectively. The diffusion coefficient for CYTC was taken as $1.33 \cdot 10^{-6}$ cm^2/s [10] and the net charge *vs.* pH table was constructed from a titration curve according to Theorell and Akesson [11] and under consideration of the charge of the iron ion (for details see ref. 12). All simulations were performed with a 1.5-cm separation space divided into 200 segments of equal length and with a constant current density of 10 A/m^2. The lengths of the focusing space and electrode compartments were 1 and 0.25 cm, respectively.

RESULTS AND DISCUSSION

An IEF_4 experiment consists of three important processes: sample injection, relaxation and elution. In order to compare the influences of different experimental conditions on retention, all fractograms are expressed in units of elution volume and not time. Comparison of fractograms of CYTC without and with an electric field applied and monitored at two detection wavelengths [280 nm (dashed lines) and 405 nm (solid lines)] is shown in Fig. 3. There is a clear difference between elution volumes of unretained (graphs 1 and 1′) and retained protein (graphs 2 and 2′). The observed difference agrees well with the theoretically expected situation because CYTC is focused in the narrower part of the channel where elution is slower (see Fig. 1A). It is

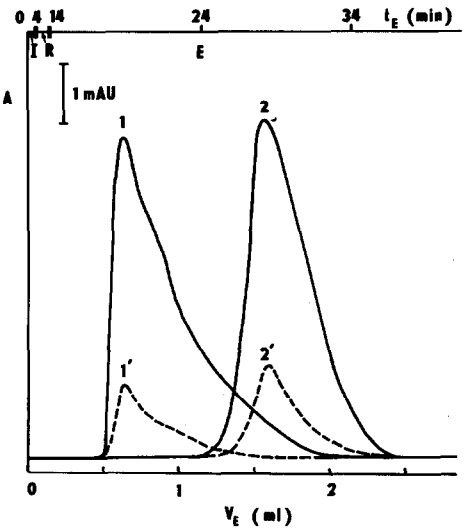

Fig. 3. Comparison of fractograms of CYTC without (1 and 1') and with (2 and 2') electric field applied and monitored at 280 nm (1' and 2') and 405 nm (1 and 2). Conditions: sample, 5 μl of $5 \cdot 10^{-5}$ *M* CYTC; carrier ampholyte solution, 0.5% (w/v) Ampholine (pH 3.5–10); electrode solutions, 0.1 *M* acetic acid (anode) and 0.1 *M* sodium hydroxide (cathode); applied voltage, 10 V; maximum current, 100 mA; relaxation time, 10 min; elution flow-rate, 100 μl/min. The time axis with the three stages, sample injection (I), relaxation (R) and elution (E), is shown at the top.

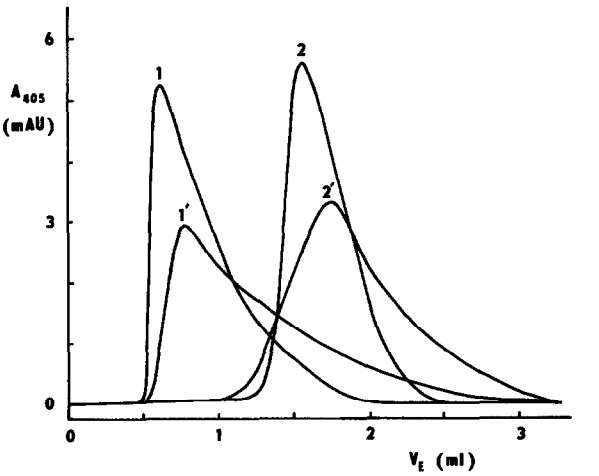

Fig. 4. Influence of different ways of sample injection on the shape of CYTC zone without (1 and 1') and with (2 and 2') electric field applied. Graphs 1 and 2 were obtained with pulse sample injection into the centre of the channel (Fig. 2B). Graphs 1' and 2' resulted from homogeneous sample injection according to Fig. 2A. Other conditions as in Fig. 3.

also evident that the detected signal is higher at 405 nm (curves 1 and 2) and, therefore, all other measurements were made at this wavelength.

Two experimental arrangements for sample injection were studied. In the first (Fig. 2A), the sample is introduced into the channel together with the ampholyte solution through the inlet capillary and its initial distribution in the inlet part of the channel is homogeneous. In the other (Fig. 2B), the sample is introduced through a capillary located 2 cm downstream from the carrier inlet. The sample is introduced as a narrow zone into the centre of the channel. The schemes of the initial distributions of components used for computer simulation and the experimental arrangements for both ways of sample injection are shown in panels a and b, respectively. As is depicted in Fig. 4, much narrower protein zones were found experimentally for the pulse sample injection both for unretained (graph 1) and retained (graph 2) CYTC compared with homogeneous sample injection (graphs 1' and 2'). In all instances the sample was focused for 10 min and then eluted at 100 μl/min.

Computer simulation data obtained with the input parameters listed under Experimental are presented in Figs. 5–7. Distributions of electrolytes and carrier ampholytes after 0, 10, 20 and 100 min of current application are shown in Fig. 5. At the beginning (A) the ampholytes are uniformly distributed throughout the focusing space, *i.e.*, the space between 0.25 and 1.25 cm of the column which is demarcated by the membranes (M). Comparison of the concentration profiles of the first two time points (A and B) reveals the progress of focusing of the ampholytes within 10 min of current flow, as well as a significant penetration of the sodium hydroxide (right-hand side) and acetic acid (left-hand side) into the focusing space. Further, some of the very acidic and very basic ampholytes are beginning to enter the electrode compartments. This is even more pronounced after 20 and 100 min of current flow (C and D, respectively), time points at which full separation of the ampholytes is predicted. These data clearly show that a relatively rapid separation phase is followed by a stabilizing phase which is characterized by a slow adjustement of the edge components (see refs. 13–15 for details).

The formation of the pH gradient (Fig. 6A) is predicted to be faster than the conductivity distribution (Fig. 6B). This is best seen by comparing the

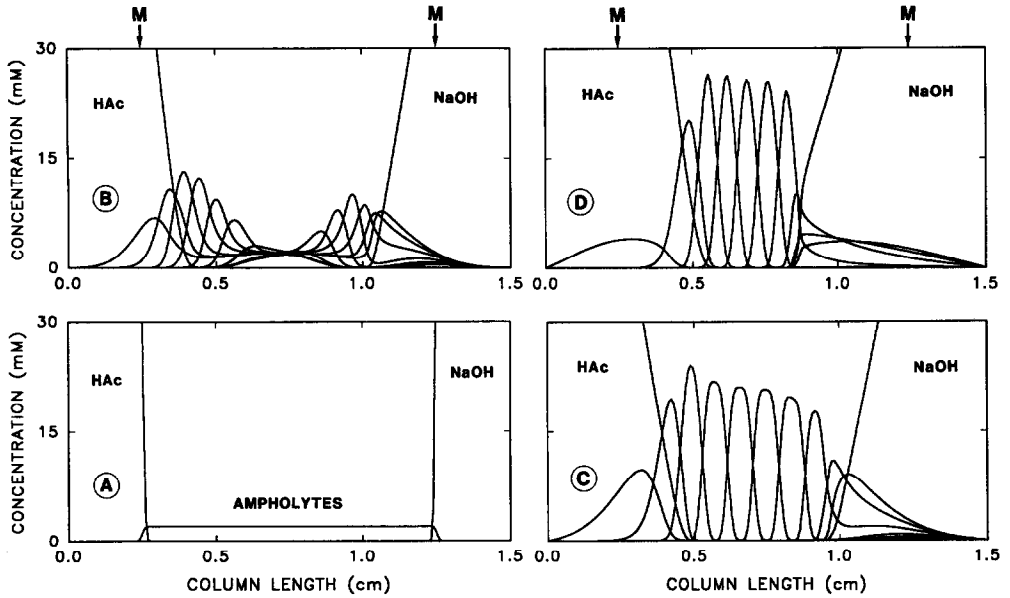

Fig. 5. Computer-simulated distribution of carrier ampholytes, anolyte (acetic acid, HAc) and catholyte (NaOH) after (A) 0, (B) 10, (C) 20 and (D) 100 min of current flow. The anode is to the left. M marks the locations of the mebranes which define the focusing space between 0.25 and 1.25 cm column length.

15-min profiles. In prolonged runs small changes can be seen especially in the neighbourhood of electrolyte chambers where the slow adjustments referred to above take place [13–15]. For the purpose of this study the most interesting results are shown in Fig. 7A and B. It is evident that focusing of a protein zone is predicted to be faster in the case of pulse sampling in the centre of the column (Fig. 7B)

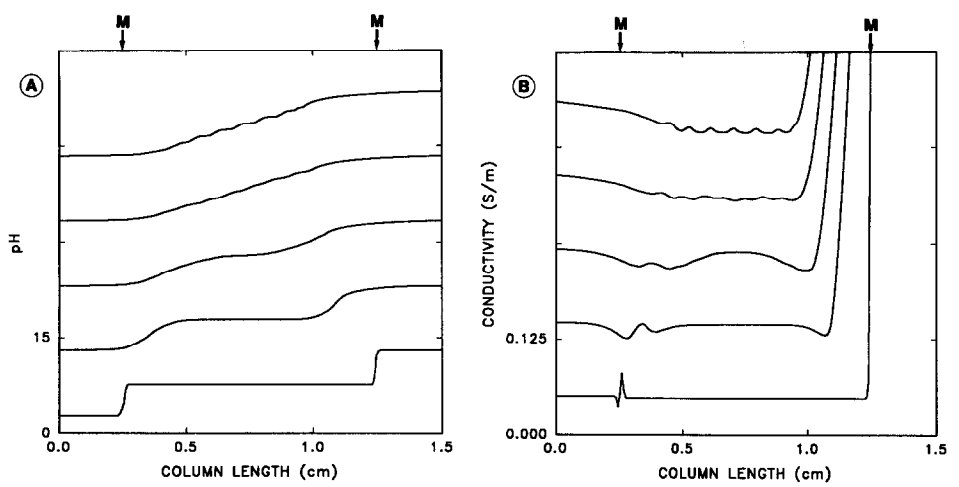

Fig. 6. Computer simulation of (A) pH gradient formation and (B) corresponding conductivity profiles after 0, 5, 10, 15 and 20 min of current flow (from bottom to top). Each successive time point is offset from the previous one by a constant amount for presentation purposes. Other conditions as in Fig. 5.

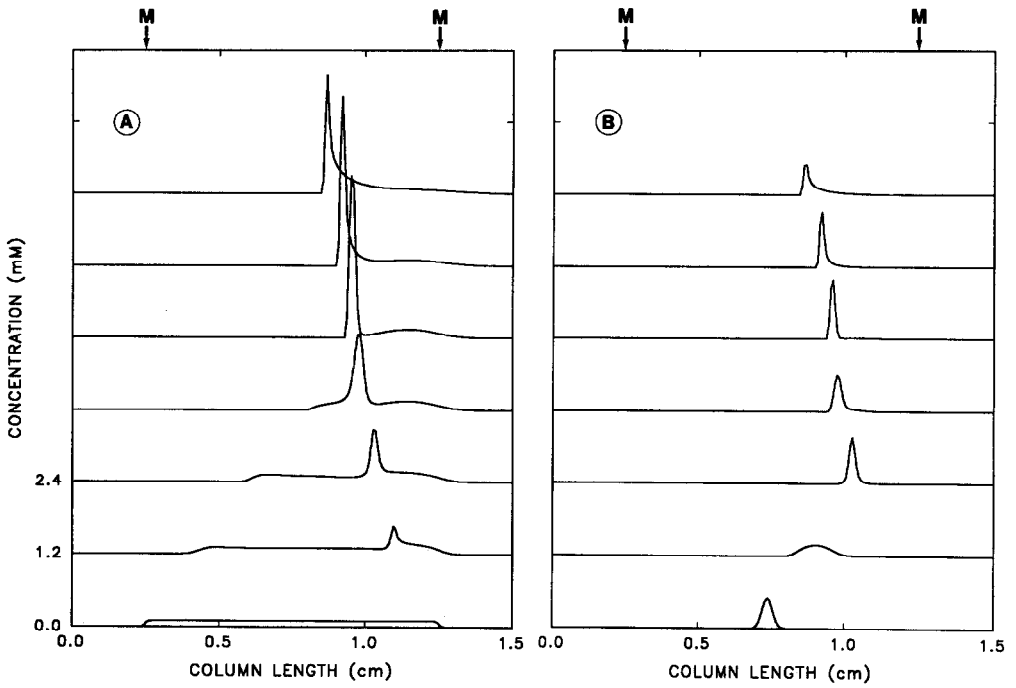

Fig. 7. Computer simulation of CYTC zone formation with (A) homogeneous sample injection (0.1 m*M*) and (B) pulse sample injection (0.5 m*M*). The initial protein distribution (bottom profiles) and offset time points after 5, 10, 15, 20, 50 and 100 min of current application are shown. Other conditions as in Fig. 5.

compared with an initial homogeneous distribution (Fig. 7A). Moreover, the transient protein zone is narrower in the former instance. Therefore, CYTC should disperse less in IEF_4 with pulse sample injection, which is exactly what is seen experimentally (Fig. 4). Another interesting finding of computer simulation is the fact that no complete steady-state distribution of CYTC is reached during 100 min of current flow. CYTC is focusing in a region where slow zone adjustements occur. However, because of the eluting nature of IEF_4, the changes between 20 and 100 min are irrelevant. There are three important conclusions for IEF_4. First, pulse sample injection (Fig. 2B) is much more efficient than homogeneous sample injection (Fig. 2A). Therefore, all remaining experiments were done with the pulse sample injection. Second, the total run time (sum of injection, relaxation and elution time intervals, see Fig. 3) should be at least 15 min, and third, focusing time >20 min only marginally influence the CYTC zone width and thus have almost no influence on the spreading of this zone during elution.

The importance of application of the electric field during sample injection is shown with the fractograms presented in Fig. 8. After sample injection the zones were immediately (without any relaxation) eluted at a flow-rate of 100 μl/min and an applied voltage of 10 V. Graph 1 shows the fractogram of CYTC injected without an applied voltage. It is evident that this broad fractogram consists of frontal and rear parts corresponding to non-retained and retained protein, respectively. With application of the electric field during sample injection only the rear part (retained) was observed (graph 2). Sample injection in the presence of the electric field resulted in a much narrower zone compared with the case of sample injection in the absence of electric field. All remaining experiments were therefore done with sample injection under an applied voltage.

The deleterious effect of the absence of the electric field during sample injection was so evident in the above experiment because no relaxation time was used after sample injection. The sample was immediately eluted at a relatively high flow-rate of 100 μl/min. The influence of relaxation time on the

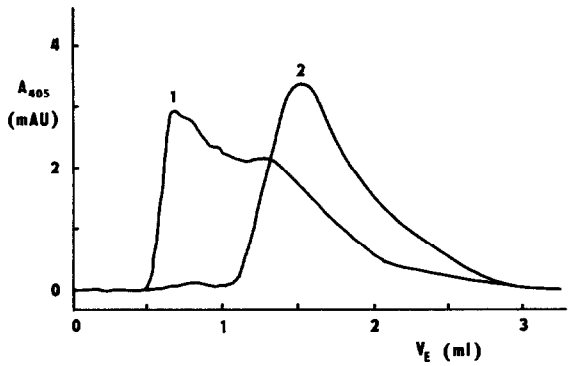

Fig. 8. Comparison of CYTC fractograms recorded without (1) and with (2) applied voltage of 10 V during sample injection. Other conditions as in Fig. 3.

elution volume of the peak maximum (V_E) and on the peak width (W_E) is shown in Fig. 9. Because of the asymmetric sample peak shape, the peak width was measured at one third of its height. It is necessary to take into account that the total focusing time during IEF_4 is the sum of the time periods of sample injection (in all instances presented this time is 4 min), relaxation (this time is variable) and elution (this time is related to the flow-rate used). It is evident from Fig. 9 that the elution volumes of the peak maxima (V_E) first increase and the peak widths decrease with higher relaxation time. The equilibrium values are reached for a relaxation time of about 10 min. This finding is in agreement with the computer simulation data.

The influence of the elution flow-rate on the shape of fractograms without and with applied voltage is shown in Fig. 10. It can be seen that the elution volumes of the peak maxima are barely influenced by different flow-rates but the peak widths increase and peak heights decrease with increasing flow-rates. The dependences of the elution times of the peak maxima and the peak widths on applied voltage and current are shown in Figs. 11A and B, respectively. The elution volumes of the peak maxima (V_E) were found to increase and the peak widths (W_E) to decrease before reaching equilibrium at a power level of about 1 W (20 V in A and 100 mA in B). Therefore, under the conditions employed and with a power < 1 W, complete focusing cannot be reached until the end of the column and transient stages are monitored. For a power exceeding 1.5 W (data not shown) the peaks became broader, indicating the occurrence of appreciable convective disturbances probably caused by Joule heating and

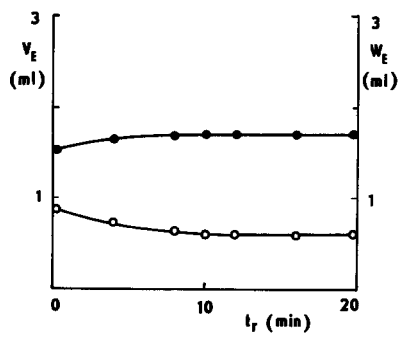

Fig. 9. Influence of relaxation time t_r, on the elution volume of the CYTC zone maximum, V_E (●), and the peak width at one third of its height, W_E (○). Other experimental conditions as in Fig. 3.

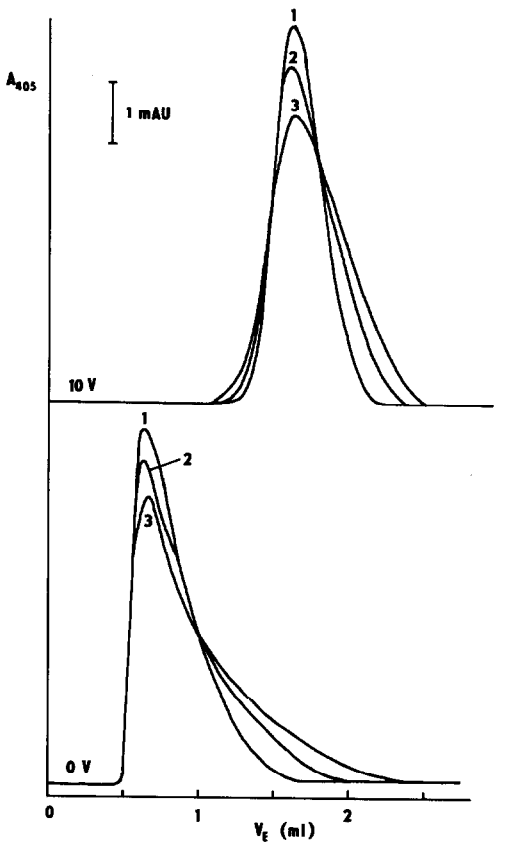

Fig. 10. Influence of the elution flow-rate on the shape of CYTC zone without (bottom) and with (top) applied power of about 1 W. Elution rates: 1 = 40; 2 = 100; 3 = 200 μl/min. Other conditions as in Fig. 3.

electrohydrodynamics. Thus, a given channel assembly with specied flow conditions should only be operated within a distinct electric power window.

CONCLUSIONS

IEF_4 of CYTC in a trapezoidal cross-sectional channel was investigated as a function of different experimental parameters, including sample injection, relaxation, elution flow-rate and applied electric power. Under the chosen conditions (pH gradient and polarity with respect to trapezoidal channel), CYTC focused in the narrower section of the channel where elution velocities are lower than in the wider part. Location of the CYTC zone is shown schematically in Fig. 1A. The observed elution volume (and of course retention time) of the retained CYTC zone was indeed found to be higher than that in absence of the electric field. Both computer simulation and experimental data showed that pulse sample injection is more efficient than homogeneous sample injection. For the described instrumental set-up it follows from the data presented that the time necessary for zone formation should be at least 15 min and that an increase in the relaxation time to >20 min does not influence the final shape of the CYTC zone. It could further be shown experimentally that the sample must be injected under an applied electric field, that the relaxation time should be about 10 min, that the elution flow-rate should not be larger than 100 μl/min and that focusing becomes more efficient with increasing electric field. The data also reveal that, under given flow conditions, the IEF_4 process should only be executed between 1 and 1.5 W, *i.e.*, within a specific power window. Investigations on the separation of proteins is the subject of another paper [12].

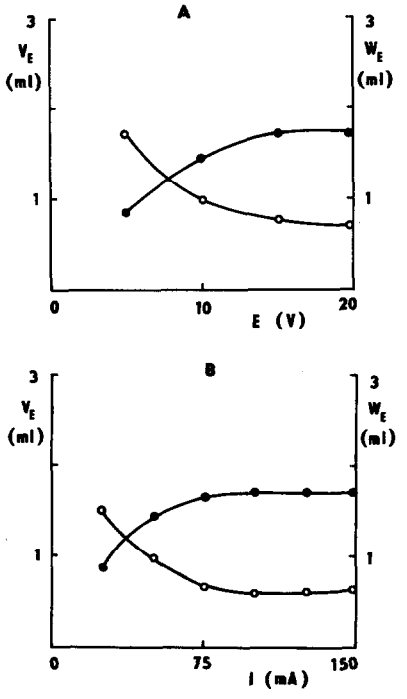

Fig. 11. Influence of applied electric power with (A) varying voltage (under a constant current of 50 mA) and (B) current (under a constant voltage of 10 V) on V_E (●) and W_E (○) of the CYTC zone. Other conditions as in Fig. 3.

ACKNOWLEDGEMENTS

The authors acknowledge the generous loan of the HPLC pump, photometric detector and recorder by Pharmacia–LKB (Bromma, Sweden). The ultrafiltration mebranes were kindly provided by Millipore (Bedford, MA, USA). This work was partly sponsored by the Swiss National Science Foundation.

REFERENCES

1 J. Janča and J. Chmelík, *Anal. Chem.*, 56 (1984) 2481.
2 J. Chmelík, M. Deml and J. Janča, *Anal. Chem.*, 61 (1989) 912.
3 W. Thormann, M. A. Firestone, M. L. Dietz, T. Cecconie and R. A. Mosher, *J. Chromatogr.*, 461 (1989) 95.
4 J. C. Giddings, *Sep. Sci. Technol.*, 18 (1983) 765.
5 J. Chmelík, *J. Chromatogr.*, 539 (1991) 111.
6 J. Chmelík, *J. Chromatogr.*, 545 (1991) 349.
7 M. Bier, O. A. Palusinki, R. A. Mosher and D. A. Saville, *Science*, 219 (1983) 1281.
8 R. A. Mosher, D. Dewey, W. Thormann, D. A. Saville and M. Bier, *Anal. Chem.*, 61 (1989) 362.
9 W. Thormann and R. A. Mosher, in C. Schafer-Nielsen (Editor), *Electrophoresis '88*, VCH, Weinheim, 1988, pp. 121–140.
10 J. T. Edsall, in H. Neurath and K. Baile (Editors), *The Proteins, Chemistry, Biological Activity and Methods*, Academic Press, New York, 1953, p. 634.
11 H. Theorell and A. Akesson, *J. Am. Chem. Soc.*, 63 (1941) 1818.
12 J. Chmelik and W. Thormann, *J. Chromatogr.*, 600 (1992) 305.
13 R. A. Mosher, W. Thormann and M. Bier, *J. Chromatogr.*, 436 (1988) 191.
14 W. Thormann and R. A. Mosher, *Adv. Electrophoresis*, 2 (1988) 47.
15 R. A. Mosher and W. Thormann, *Electrophoresis*, 11 (1990) 717.